



Design and Investigation of a Thermoelastic Actuator with Tailored Unidirectional Thermal Expansion and Stiffness using Mechanical Metamaterials and Joule Heating Activation

Erhard Buchmann¹(✉), Isabel Prestes², Bruno Musil¹, and Philipp Höfer¹

¹ Universität der Bundeswehr München, Institute of Lightweight Engineering, Neubiberg, Germany

{erhard.buchmann,bruno.musil,philipp.hoefer}@unibw.de

² Universität der Bundeswehr München, Institute of Materials Science, Neubiberg, Germany

isabel.prestes@unibw.de

Abstract. Mechanical metamaterials have become an emerging research field due to the advances in additive manufacturing technology in the last decade. Especially, materials with adjustable coefficient of thermal expansion (CTE)—thermoelastic metamaterials—are investigated because of their wide range of engineering applications. They span from the shape control of space structures to micro positioning systems. For designing the CTE of metamaterials, at least two materials with different CTEs have to be combined in complex lattice structures, which makes manufacturing difficult up to now. However, with the advent of multi-material additive manufacturing such metamaterials become available. Extensive research examined topological designs of passive thermoelastic unit cells. Regarding topological concepts for applications as actuator, mainly only homogeneous temperature differences and mechanical forces as activation have been addressed. However, the activation through joule heating is addressed rarely. In this work, the design of a bi-metallic thermoelastic actuator based on mechanical metamaterials with joule heating activation is presented. First, an efficient parameterization for the underlying triangular metamaterial cell with double-coned legs inspired by pentamode metamaterials is presented. The cell design concept is investigated using finite element method regarding stiffness and CTE as well as their coupling and the influence of the double cone shape of the legs. Second, two principal design options for the accommodation of foil heaters on the actuator cell are compared. By using a transient simulation of an actuator consisting of a tessellation of the designed cells, the thermoelastic functionality could be shown.

Keywords: Metamaterial · Smart materials · Thermal Expansion · Additive Manufacturing · Multi-Material · Actuator · Thermoelasticity

1 Introduction

Most of the natural materials expand with the rise of temperature and shrink by decreasing it, which characterizes them as materials with positive coefficient of thermal expansion (CTE). In contrast, near-zero CTEs and even negative CTEs are intrinsic properties of few materials for specific temperature ranges [1–3]. Also, these materials generally have a limited mechanical performance, which limits their engineering applications [2, 4].

These limitations of natural negative CTE materials can be overcome with mechanical metamaterials. Mechanical metamaterials show a rationally architected micro structure that results in a desired macroscopic behavior [5]. This includes auxetic metamaterials that present a negative Poisson’s ratio, pentamode metamaterials where arbitrary anisotropic stiffnesses can be obtained and thermoelastic metamaterials where a tunable CTE can be reached [2, 6–9]. Thermoelastic metamaterials with controllable CTE have been investigated for over 20 years [10, 11]. Structures with high unidirectional CTE are desired for actuators controlled by temperature, while structures with zero, minimal or even negative CTE are intended especially for applications that either involve high temperature variations or require high dimensional accuracy, or both [4, 12, 13]. Applications reach from high-precision spaceborne optical systems to microchip devices [4, 14–17]. For the sake of achieving these properties, these microstructures must have specific geometries and must be composed of at least two different materials with a CTE difference among them [18]. With the advent of metallic multi-material additive manufacturing they become available for structural applications [19–22].

Recent studies focus on the one hand on metamaterials that present a controllable CTE and yet are structurally efficient [12, 13, 23–27]. On the other hand, stimuli-responsive thermoelastic metamaterials called actuators [28], active metamaterials [29] and 4D thermomechanical metamaterials [30] are investigated. The underlying metamaterial ground structures usually work with flexure joints instead of applying structurally efficient double-cone struts of pentamode metamaterials [31–33]. Moreover, besides an activation via heating the whole actuator [24, 28, 31, 32, 34], only limited studies consider a local activation. In [35] a micro actuator activated by a laser with triangular displacement amplification is investigated. In [36] and [37] additively manufactured actuators that are activated by a standard foil heater are investigated. In the work, the thermoelastic functionality could be shown in simulations and experiments. However, no multi-metamaterial actuators are investigated there.

In this study, the design of a planar bi-metallic thermoelastic actuator cell applying mechanical metamaterials with joule heating activation is presented. For investigation, a parameterized geometry based on a bi-material triangle with double cone legs inspired by pentamode metamaterials is utilized. The parameters’ effect on the stiffness and the CTE as well as their coupling are evaluated. Moreover, two options for the joule heating activation with a standard foil heater that requires a minimal surface area are compared: by thickening the middle strut and by applying an additional out-of-plane accommodation structure.

2 Design of the Thermoelastic Actuator Cell

2.1 Negative Thermal Expansion Mechanism of the Actuator Cell

The negative thermal expansion (NTE) of the unit cells of thermoelastic metamaterials is based on a purposefully designed geometric structure using at least two different materials with a preferably large CTE-difference [18]. These geometric structures can be classified in bending-dominated and stretch-dominated according to the underlying expansion mechanism. In this work, a stretch-dominated structure is applied as it is structurally more efficient compared to a bending-dominated structure and therefore more suitable for engineering applications [38–40]. In Fig. 1, a scheme of the applied triangular deformation mechanism of the used planar unit cell for unidirectional expansion in y -direction is shown. When heated by the temperature ΔT , the thermal elongation in axial direction of the middle strut $a - a_0$ is higher than the elongation of the legs due to its higher CTE. This results in a rotation of the legs by the angle $\varphi_0 - \varphi$. Thus the height of the triangular structure h_0 decreases to h . The resulting elongation in y -direction will be henceforth called the structure's CTE, which is calculated by $CTE = (h_0 - h)/(h_0 \Delta T)$. Besides, the stiffness is defined with respect to a unit force F in y -direction. The CTE and the stiffness of this actuator cell are majorly determined by the edge length a and the angle φ . These properties are highly coupled. For instance, low angles lead to high NTEs and low stiffness in y -direction at the same time. Remarkably, actuators with high positive CTE can be built by reversing the high- and low-CTE material.

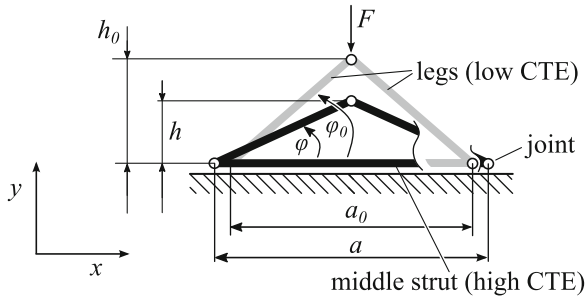


Fig. 1. Scheme of the underlying planar triangular mechanism with idealized rotational joints for a unidirectional negative thermal expansion in y -direction. When heated, the thermal elongation in axial direction of the middle strut $a - a_0$ is higher than the elongation of the legs due to its higher CTE. This leads to a rotation of the legs by the angle $\varphi_0 - \varphi$ resulting in a decrease in height from h_0 to h . The stiffness is defined with respect to a unit force F in y -direction.

2.2 Design Objectives and Parametrization of the Geometry of the Actuator Cell

In this work, a concept for an actuator for engineering applications, especially space applications, is presented. The process of 3D multi-material L-PBF is

particularly suitable to fabricate these structures. However, the metallic multi-material L-PBF is not yet a consolidated process. Consequently, there are some design restrictions and the choice for a simplified design, where no or minimal support structures are required, is convenient. The following design objectives are taken into account here:

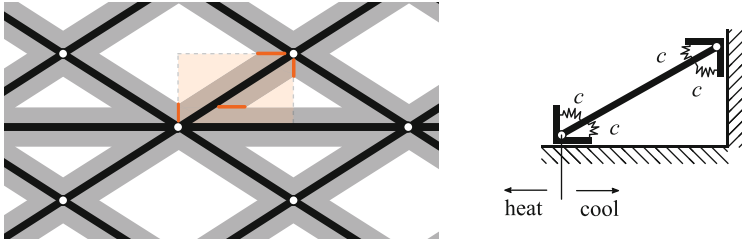
- High Stiffness in y -direction
- High NTE in y -direction
- Joule heating activation with a standard foil heater
- Good manufacturability with bi-material metallic additive manufacturing

When implementing the presented triangular mechanism, a certain wall thickness is required because of stiffness and process requirements. Moreover, in applications actuator cells are usually connected in series for higher NTEs or in parallel for higher stiffnesses. This results in an overlapping of the thicknesses of the struts at the joints as depicted in Fig. 2a. Accordingly, additional rotational stiffness arise (see Fig. 2b). This especially applies for very small angles.

However, the triangular mechanism creating the NTE requires a rotation in the joints. Accordingly, a geometric parametrization with double-coned legs is applied. The smaller thickness at the joints reduces rotational stiffness while in the middle of the strut a high bending resistance preventing buckling of the legs is kept (see Fig. 3) [7–9]. Due to the high complexity with manufacturing structurally more efficient tubular structures are not considered here. The middle strut is not tapered since there the foil heater is attached. The overall thickness t_1 is applied. In order to provide enough space for the accommodation of a foil heater, the middle strut can be thickened (m). For the legs, the thickness t_1 is reached only in the middle of the strut while the ends are tapered. At the ends of the legs, the thicknesses t_2 and $t_2/2$ are applied. The $t_2/2$ -offset at the left corner is important for the avoidance of overlapping of the legs with the middle strut at very small angles. The angle φ is defined from the middle strut middle axis to the leg middle axis.

When considering wall thicknesses, there are two main mechanisms of thermal expansion that counteract when aiming for high NTEs:

- Geometric nonlinear triangular thermal expansion mechanism
- Thermal expansion of the structure in y -direction defined by the geometric expansion in y -direction h_l and h_h .



(a) Tesselation of the actuator cell. Idealized lattice model with rotational pin joints (black). Compliant mechanism considering the wall thickness (grey). Arise of additional rotational stiffnesses (orange) illustrated in a quarter cell (dotted).

(b) Illustration of the arising rotational stiffnesses c when considering the wall thickness using a quarter model.

Fig. 2. Arising rotational stiffness of the actuator cell when taking wall thickness into account.

2.3 Joule Heating Activation

For the joule heating activation, commercially available foil heaters are utilized. This is especially applicable for space application where space-qualified heaters are preferred. Therefore, multi-hierarchically and small-scale structures are not suitable as an activation with standard heaters is difficult. For foil heaters, a minimum space for accommodation is required due to the maximum power intensity (approx. $0.5 \frac{\text{W}}{\text{cm}^2}$ [41]) and the minimum width. Consequently, for the accommodation of the foil heaters the middle strut is preferable over the legs since it is longer. Moreover, activating the middle strut instead of the legs makes the actuator more efficient because it results in a higher temperature in the middle strut than in the legs. This results in a higher decrease in height due to the higher difference in thermal elongation.

For the increase in width two option are investigated here:

- Joule heating activation by thickening the middle strut (see Fig. 4a)
- Joule heating activation with an additional accommodation structure attached to the middle strut (see Figs. 4b and 4c)

In the first option, not only a foil heater could be directly attached to the middle strut, but also a heating cartridge could be accommodated inside it, as depicted in Fig. 4a. However, the thickening of the middle strut leads to lower NTE. Due to its higher and isotropic CTE, the elongation of the middle strut would cause a higher elongation in the y -direction as well. Therefore, an out-of-plane structural enlargement for the accommodation is applied in the second option. Here, an exemplary double cone and a plate are depicted, whereby other geometries could be utilized. The plate is not suitable for low edge lengths.

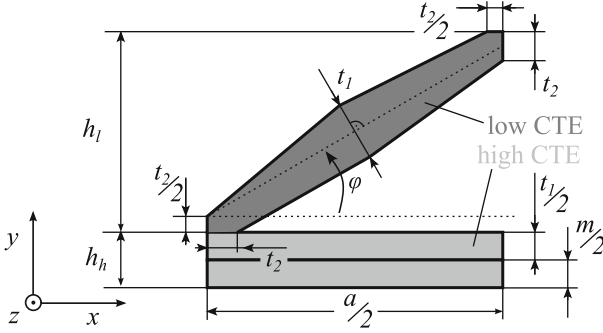
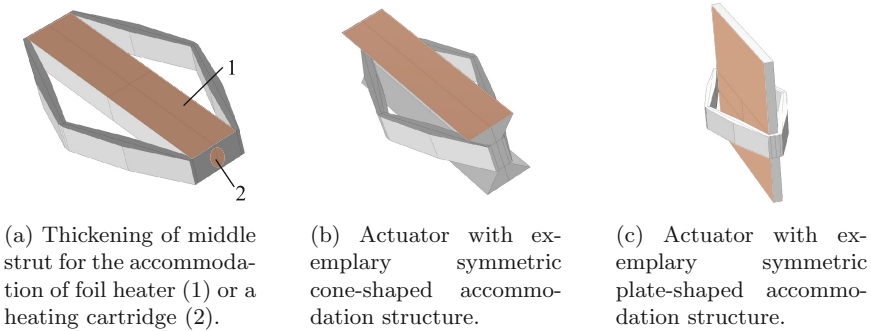


Fig. 3. Quarter model of the parametrization of the geometry with double cone legs and with a thickening of the middle strut (m) for the accommodation of a foil heater.



(a) Thickening of middle strut for the accommodation of foil heater (1) or a heating cartridge (2). (b) Actuator with exemplary symmetric cone-shaped accommodation structure. (c) Actuator with exemplary symmetric plate-shaped accommodation structure.

Fig. 4. Options for the accommodation of a foil heater (orange).

3 Investigation of the CTE and the Stiffness of the Actuator Cell

For the evaluation of the actuator cell, CTE, stiffness and their coupling as well as the efficiency of both joule heating activation options are investigated using finite element method. To this, different sets of parameters were investigated in Sect. 3.1, 3.2, 3.3, 3.4 and 4. An overview of the applied parameter sets and the materials can be found in Tables 1 and 2. Steel was applied as the high CTE material and Invar as the low CTE material. Both are structurally efficient while having a considerably large CTE gap. Moreover, bi-material powder bed fusion is feasible using them because of the good weldability of both materials [42, 43]. All investigations are done under the variation of the angle φ in an interval of $[6^\circ; 60^\circ]$ using a 2.5 mm thick model. First, the influence of the main parameters a , φ and t is studied. Then, the influence of the double cone shape of the legs and the influence of the thickening of the middle strut is investigated.

Table 1. Overview over parameters applied for the investigations.

Section	t_1 [mm]	t_2 [mm]	m [mm]	a [mm]	φ [°]
3.1		[0.5; 1.5]	0	[10; 20]	
3.2	1	[0.5; 1]	0		
3.3	1	1	0	20	[6; 60]
	1	0.5	0		
3.4	1	0.5	[0; 10]		
4	1	0.5	0	20	20
	1	0.5	3		

Table 2. Material parameters and thickness in z -direction.

Parameter	Unit	Steel	Invar
Young's modulus	GPa	200	140
Poisson's ratio	–	0.3	0.3
CTE	$10^{-6}1/K$	18	1
Thermal conductivity	$\frac{W}{m \cdot K}$	15	13.5
Heat capacity	$\frac{J}{kg \cdot K}$	510	515
Density	$\frac{kg}{m^3}$	7900	8100
Thickness in z -direction	mm		2.5

3.1 Influence of the Edge Length a and the Overall Thickness $t_{1,2}$

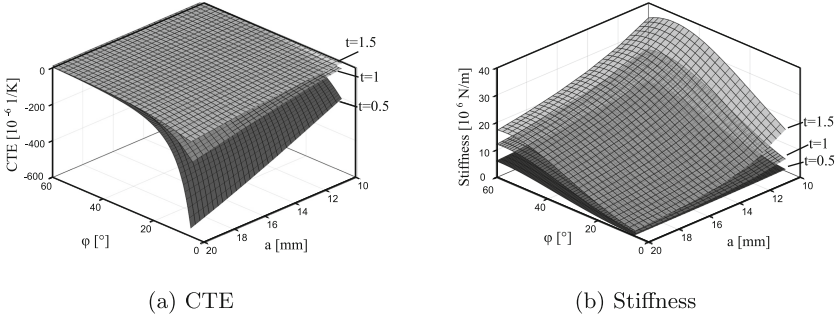
The influence of the edge length a and the overall thickness under different angles was investigated (see Fig. 5). Both parameters greatly influence the CTE and the stiffness: A higher NTE is generated by lower angles, smaller thicknesses and higher edge lengths (see Fig. 5a). By contrast, a higher stiffness results from higher angles, higher thicknesses and lower edge lengths (see Fig. 5b). Consequently, as a rule of thumb, the stiffness and CTE are of competing interest (see Table 3).

However, regarding the CTE, only for angles smaller than approx. 20° a considerable strong effect for the NTE can be observed. In this course, an increase in thickness reduces this effect.

Regarding the stiffness, there is a decrease for angles greater than approx. 50° due to the activation of bending deformation in the legs. This effect is also stronger for shorter edge lengths and could be hindered by using higher thicknesses in the middle of the legs. However, this effect is not considered any further as the focus of this work is on structures with high NTE that require long edges and small angles.

Table 3. Contradicting influence of the geometric parameters φ , a , $t_{1,2}$ on stiffness and NTE.

Design objective	Parameter		
	φ	$t_{1,2}$	a
Stiffness	↑	↑	↓
NTE	↓	↓	↑

**Fig. 5.** Influence of the edge length a and the overall thickness t on the stiffness and CTE of the actuator cell under variation of the angle φ .

3.2 Influence of the Double Cone Shape of the Legs

In a second step, the influence of the double cone shape of the legs under different angles was investigated (see Fig. 6). To do this, a reduction of t_2 from 1 mm to 0.5 mm was considered while keeping $t_1 = 1$ mm and $a = 20$ mm. It was observed, that a higher tapering results in a much higher NTE while having a minor effect on the stiffness. This especially applies for smaller angles φ . Consequently, tapering the legs is well suited to improve the actuator geometry when taking the design objectives stiffness and CTE into account at the same time. Due to the definition of the CTE-stiffness-relationship using only two variables, this parametrization is well suited for a fast preliminary design of components with many coupled cells followed by a topology optimization for detailed design.

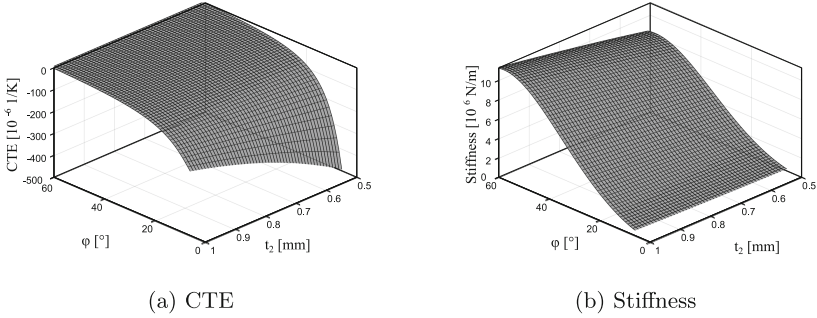


Fig. 6. Influence of the tapering of the legs (defined by t_2) on the stiffness and CTE of the actuator cell under variation of the angle φ . A constant thickness $t_1 = 1$ mm and a constant edge length $a = 20$ mm is applied.

3.3 Comparison of Actuator Cells with Tapered and Non-Tapered Legs

Third, a tapered ($t_2 = 0.5$ mm) and a non-tapered ($t_2 = 1$ mm) actuator cell with a constant edge length $a = 20$ mm and a constant width of $t_1 = 1$ mm were comparatively examined under the variation of the angle φ (see Fig. 7). The influence of the tapering varies under different angles φ : For decreasing angles the effect on the NTE rises while the impact on the stiffness decreases. This is due to the higher overlapping of the legs with the middle strut when considering thicknesses which can be overcome by the tapering (see Fig. 7). Thus, the double cone shape of the legs is beneficial for the actuator design where high NTEs that require low angles and high stiffnesses are to be reached simultaneously. Nevertheless, only pareto-optimal solutions can be achieved in terms of stiffness and NTE. The decrease in stiffness for angles higher than approx. 55° depicted in Fig. 5b can also be seen here.

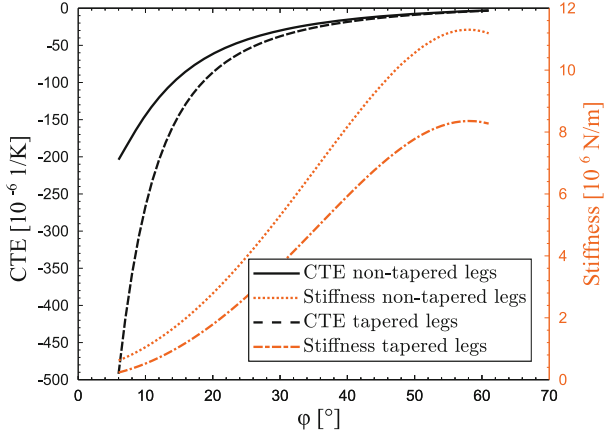


Fig. 7. Comparison of an actuator cell with tapered and non-tapered legs under the variation of the angle φ . A constant thickness $t_1 = 1$ mm and a constant edge length $a = 20$ mm is applied.

3.4 Influence of the Thickening of the Middle Strut on the CTE

Fourth, the influence of thickening of the middle strut (defined by m) on the CTE is investigated (see Fig. 8). To do this, an actuator cell with tapered legs ($t_2 = 0.5$ mm) with a constant edge length $a = 20$ mm and a constant width of $t_1 = 1$ mm was studied under the variation of the angle φ . It can be observed that higher thicknesses of the middle strut result in significantly lower NTEs. This effect is due the higher geometric expansion in y -direction (h_h) resulting in a higher thermal expansion in y -direction which counteracts the triangular expansion mechanism (see Fig. 3). Thus, for example, at an angle $\varphi = 20^\circ$, the actuator cell has a CTE of approx. $-9 \cdot 10^{-6}$ 1/K with no thickening of the middle strut ($m = 0$ mm) while there is a CTE of approx. $-3 \cdot 10^{-6}$ 1/K for $m = 10$ mm. As a consequence, the thickening of the middle strut is only suitable for the joule heating activation when small NTEs are sufficient. However, it is advantageous that no support structures are needed at additive manufacturing using this type of activation.

4 Investigation of the Transient Thermal Expansion Applying Joule Heating Activation

For the investigation of the transient thermal expansion an actuator cell tessellation comparing both joule heating activation options is considered (see Figs. 9a and 9b). By applying a tessellation, a higher overall negative expansion can be achieved. Moreover, by using two rows of cells next to each other, the actuator is stiffer, in particular regarding multiaxial loads. The same size of activation surface with a watt density of $0.5 \frac{W}{cm^2}$ is applied on front- and backside for

both options and the displacement u after 10s is evaluated. The scale of the displacements is in μm -scale for both options which is suitable for spaceborne (see Fig. 9c). However, when applying a double cone as accommodation structure for the foil heater far higher negative displacements can be reached especially at small angles.

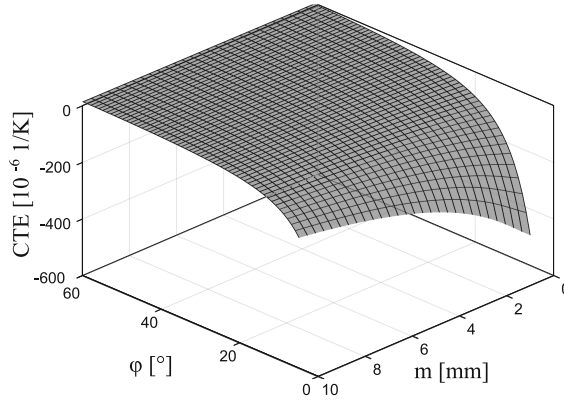
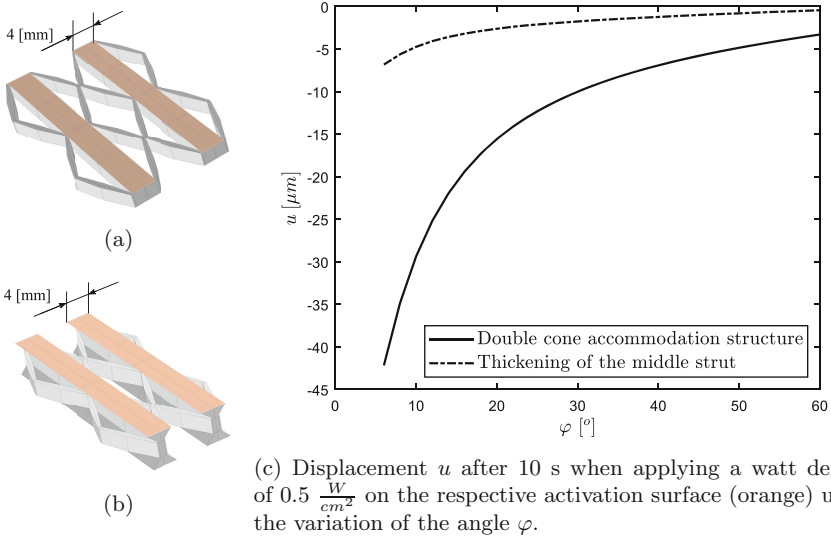


Fig. 8. Influence of the thickening of the middle strut on the CTE under the variation of the angle φ .



(c) Displacement u after 10 s when applying a watt density of $0.5 \frac{\text{W}}{\text{cm}^2}$ on the respective activation surface (orange) under the variation of the angle φ .

Fig. 9. Comparison of the transient thermal expansion of an actuator cell tessellation with joule heating activation using a thickening of the middle strut (9a) and a double cone (9b).

5 Conclusion

In this work, the design of a bi-metallic thermoelastic actuator with negative thermal expansion (NTE) based on mechanical metamaterial with joule heating activation was presented. First, an efficient parametrization of the actuator cell based on a triangular geometry where double-cone-shaped legs can be considered, is presented. The stiffness and CTE were then investigated and it was observed that both are highly coupled, but contradict design objectives regarding the geometric parameters $\varphi, a, t_{1,2}$. This contradiction, however, can be overcome using tapered legs. At the end, two options for the joule heating activation which requires a certain width were investigated: by thickening the middle strut and by applying an out-of-plane structural enlargement. It was shown that the latter is suitable to reach higher negative displacements. On the other hand, the AM of these structures would require support structures. In future work, the thickness at the bi-material interface could be studied taking in consideration the strength of the weld seam. Moreover, the stiffnesses and CTEs in arbitrary directions can be taken into account as design objectives. The presented actuator has a high potential for applications in actively controlled satellite structures [44].

Acknowledgements. This work within the project SeRANIS is funded by dtcc.bw—Digitalization and Technology Research Center of the Bundeswehr which we gratefully acknowledge. dtcc.bw is funded by the European Union—NextGenerationEU.

References

1. Miller, W., Smith, C., Mackenzie, D., Evans, K.: Negative thermal expansion: a review. *J. Mater. Sci.* **44**(20), 5441–5451 (2009)
2. Takenaka, K.: Negative thermal expansion materials: Technological key for control of thermal expansion. *Sci. Technol. Adv. Mater.* (2012)
3. Barrera, G.D., Bruno, J.A.O., Barron, T., Allan, N.: Negative thermal expansion. *J. Phys. Condens. Matter.* **17**(4), R217 (2005)
4. Jefferson, G., Parthasarathy, T.A., Kerans, R.J.: Tailorable thermal expansion hybrid structures. *Int. J. Solids Struct.* **46**(11–12), 2372–2387 (2009)
5. Zadpoor, A.A.: Mechanical meta-materials. *Mater. Horiz.* **3**(5), 371–381 (2016)
6. Joseph, A., Mahesh, V., Harursampath, D.: On the application of additive manufacturing methods for auxetic structures: a review. *Adv. Manuf.* **9**(3), 342–368 (2021)
7. Milton, G.W., Cherkaev, A.: Which elasticity tensors are realizable. *J. Eng. Mater. Technol. Trans. Asme* **117**, 483–493 (1995)
8. Kadic, M., Bückmann, T., Stenger, N., Thiel, M., Wegener, M.: On the practicality of pentamode mechanical metamaterials. *Appl. Phys. Lett.* **100**(19), 191901 (2012)
9. Akbari, M., Mirabolghasemi, A., Bolhassani, M., Akbarzadeh, A., Akbarzadeh, M.: Strut-based cellular to shellular funicular materials. *Adv. Funct. Mater.* **32**(14), 2109725 (2022)
10. Lakes, R.: Cellular solid structures with unbounded thermal expansion. *J. Mater. Sci. Lett.* **15**(6), 475–477 (1996)

11. Sigmund, O., Torquato, S.: Composites with extremal thermal expansion coefficients. *Appl. Phys. Lett.* **69**(21), 3203–3205 (1996)
12. Lakes, R.: Cellular solids with tunable positive or negative thermal expansion of unbounded magnitude. *Appl. Phys. Lett.* **90**(22), 221905 (2007)
13. Lehman, J., Lakes, R.S.: Stiff, strong, zero thermal expansion lattices via material hierarchy. *Compos. Struct.* **107**, 654–663 (2014)
14. Guo, X., Ni, X., Li, J., Zhang, H., Zhang, F., Yu, H., Wu, J., Bai, Y., Lei, H., Huang, Y., et al.: Designing mechanical metamaterials with kirigami-inspired, hierarchical constructions for giant positive and negative thermal expansion. *Adv. Mater.* **33**(3), 2004919 (2021)
15. Li, X., Gao, L., Zhou, W., Wang, Y., Lu, Y.: Novel 2d metamaterials with negative poisson's ratio and negative thermal expansion. *Extreme Mech. Lett.* **30**, 100498 (2019)
16. Lim, T.C.: Negative thermal expansion structures constructed from positive thermal expansion trusses. *J. Mater. Sci.* **47**(1), 368–373 (2012)
17. Raminhos, J., Borges, J., Velinho, A.: Development of polymeric anepctic meshes: Auxetic metamaterials with negative thermal expansion. *Smart Mater. Struct.* **28**(4), 045010 (2019)
18. Kalamkarov, A.L., Kolpakov, A.G.: Analysis, design and optimization of composite structures, vol. 1. Wiley, New York (1997)
19. Anstaett, C., Seidel, C., Reinhart, G.: Fabrication of 3d multi-material parts using laser-based powder bed fusion. In: 2017 International Solid Freeform Fabrication Symposium. University of Texas at Austin (2017)
20. Girth, S., Koopmann, J., Klawitter, G., Waldt, N., Niendorf, T.: 3d hybrid-material processing in selective laser melting: Implementation of a selective coating system. *Prog. Addit. Manuf.* **4**(4), 399–409 (2019)
21. Schneck, M., Horn, M., Schmitt, M., Seidel, C., Schlick, G., Reinhart, G.: Review on additive hybrid-and multi-material-manufacturing of metals by powder bed fusion: State of technology and development potential. *Progress in Additive Manufacturing* pp. 1–14 (2021)
22. Neirinck, B., Li, X., Hick, M.: Powder deposition systems used in powder bed-based multimetal additive manufacturing. *Acc. Mater. Res.* **2**(6), 387–393 (2021)
23. Ai, L.: Micro-architected Metamaterials: Design and Analysis. Ph.D. thesis, Southern Methodist University (2017)
24. Wei, K., Chen, H., Pei, Y., Fang, D.: Planar lattices with tailorable coefficient of thermal expansion and high stiffness based on dual-material triangle unit. *J. Mech. Phys. Solids* **86**, 173–191 (2016)
25. Xu, H., Pasini, D.: Structurally efficient three-dimensional metamaterials with controllable thermal expansion. *Sci. Rep.* **6**(1), 1–8 (2016)
26. Li, J., Liu, H.T., Zhang, Z.Y.: Stiffness characteristics for bi-directional tunable thermal expansion metamaterial based on bi-material triangular unit. *Int. J. Mech. Sci.* **241**, 107983 (2023)
27. Xu, M., Zhao, Z., Wang, P., Zhang, Y., Guo, X., Lei, H., Fang, D.: Planar bi-metallic lattice with tailorable coefficient of thermal expansion. *Acta Mech. Sinica* **38**(7), 1–9 (2022)
28. Sigmund, O.: Design of multiphysics actuators using topology optimization-part ii: Two-material structures. *Comput. Methods Appl. Mech. Eng.* **190**(49–50), 6605–6627 (2001)
29. Qi, J., Chen, Z., Jiang, P., Hu, W., Wang, Y., Zhao, Z., Cao, X., Zhang, S., Tao, R., Li, Y., et al.: Recent progress in active mechanical metamaterials and construction principles. *Adv. Sci.* **9**(1), 2102662 (2022)

30. Ji, Q., Moughames, J., Chen, X., Fang, G., Huaroto, J.J., Laude, V., Martínez, J.A.I., Ulliac, G., Clévy, C., Lutz, P., et al.: 4d thermomechanical metamaterials for soft microrobotics. *Commun. Mater.* **2**(1), 1–6 (2021)
31. Taniker, S., Celli, P., Pasini, D., Hofmann, D., Daraio, C.: Temperature-induced shape morphing of bi-metallic structures. *Int. J. Solids Struct.* **190**, 22–32 (2020)
32. Xu, H., Farag, A., Ma, R., Pasini, D.: Thermally actuated hierarchical lattices with large linear and rotational expansion. *J. Appl. Mech.* **86**(11) (2019)
33. Song, C., Li, S., Bao, H., Ju, J.: Design of thermal diodes using asymmetric thermal deformation of a kirigami structure. *Materials & Design* **193**, 108734 (2020)
34. Buchmann, E., Hadwiger, F., Petroll, C., Zauner, C., Horoschenkoff, A., Höfer, P.: A unit cell with tailorable negative thermal expansion based on a bolted additively manufactured auxetic mechanical metamaterial structure: Development and investigation. In: *Proceedings of the Munich Symposium on Lightweight Design 2021*. pp. 198–211. Springer (2023)
35. Parreira, R., Özelçi, E., Sakar, M.S.: Investigating tissue mechanics in vitro using untethered soft robotic microdevices. *Front. Robot. AI* **8**, 649765 (2021)
36. Cho, Y., Lee, E., Kim, Y.: Design and performance evaluation of retraction-type actuators with displacement amplification mechanism based on thermomechanical metamaterial. *J. Aerosp. Sys. Eng.* **14**(2), 28–35 (2020)
37. Jo, Y., Lee, E., Kim, Y.: Design and performance evaluation of extension-type actuators with a displacement amplification mechanism based on chevron beam. *J. Aerosp. Sys. Eng.* **15**(6), 1–9 (2021)
38. Xu, H., Farag, A., Pasini, D.: Routes to program thermal expansion in three-dimensional lattice metamaterials built from tetrahedral building blocks. *J. Mech. Phys. Solids* **117**, 54–87 (2018)
39. Steeves, C.A., e Lucato, S.L.d.S., He, M., Antinucci, E., Hutchinson, J.W., Evans, A.G.: Concepts for structurally robust materials that combine low thermal expansion with high stiffness. *J. Mech. Phys. Solids* **55**(9), 1803–1822 (2007)
40. Cardoso, J.O., Borges, J.P., Velinho, A.: Structural metamaterials with negative mechanical/thermomechanical indices: A review. *Prog. Nat. Sci.: Mater. Int.* (2021)
41. Schlitt, R., Kuhlmann, S., Sander, B., Neustadt, S.: Assessment of the rules on heater de-rating. *ESA Space Passive Component Days* (2016)
42. Arbogast, A., Roy, S., Nycz, A., Noakes, M.W., Masuo, C., Babu, S.S.: Investigating the linear thermal expansion of additively manufactured multi-material joining between invar and steel. *Materials* **13**(24), 5683 (2020)
43. Zhan, X., Zhu, Z., Yan, T., Gao, Q., Liu, Z.: The influences of different filler metals on the microstructure of invar fe-36ni alloy multi-layer multi-pass mig welding. *Mater. Res. Express* **6**(2), 026555 (2018)
44. Möller, F., Essig, T., Holzhauer, S., Förstner, R.: Experimental demonstration of a method to actively stabilize satellite structures against random perturbations of thermal boundary conditions using a closed-loop filter and controller approach. *CEAS Space Journal* pp. 1–18 (2023)